Impact of 3D magnetic perturbations on turbulent transport in tokamak limited plasmas

B. Luce[1,2], P. Tamain[2], G. Ciraolo[2], E. Serre[1], C. Baudoin[1], H. Bufferand[2], T. Cartier-Michaud[1], Ph. Ghendrih[2], E. Laribi[2], F. Schwander[1], and R. Tatali[1]

[1] *Aix-Marseille Université, CNRS, Centrale Marseille, M2P2, Marseille, France*
[2] *CEA, IRFM, F-13108, St Paul-lez-Durance, France*

benjamin.luce@univ-amu.fr

Abstract

A 3D fluid code for edge plasma has been used to study the impact of several amplitude-varying magnetic perturbations (MP) on transport and turbulence. Assuming the vacuum approximation, an eletrostatic and isothermal model, we note a flow reorganization, in particular the increase of the radial electrical field in closed field line region (CFLR), in qualitative agreement with experiments, and a change in response of parallel flows. We observe a density pump-out (loss of density) with fine effects on the radial transport. The complex behaviour of the turbulence shows an increase of its intensity with the amplitude of the perturbation but not correlated with the variation of the density pump-out. An analyze of the Scrape-off layer (SOL) density decay length shows a decrease of the latter with the increasing amplitude of magnetic perturbations.

1 Introduction

A Tokamak has theoretically an axisymmetric magnetic field. However, the magnetic field is never perfectly homogeneous in the toroidal direction. These non-axysimmetries are more of a critical topic as what one may think as even a small perturbation of the order of $\delta B \sim 10^{-4} B_\varphi$ can cause significant change of the plasma behaviour [1, 2]. The 2 most common reasons for non-axisymmetrical fields are engineering limitations and artificial perturbations applied by additional coils for control purposes. The latter are planned to be used in ITER to mitigate and/or suppress Edge Localized Modes (ELMs) via Resonant Magnetic Perturbations (RMPs) [3].

Experiments on current machines have shown the capability of RMPs to achieve their purpose but have also demonstrated an impact on the edge plasma equilibrium as well as on turbulence [4–7]. One of the concerns for futur devices is the consequences on the particle and heat flux distributions on the targets. A review of RMP effect on edge plasma can be seen in [2] and references herein. Summarizing briefly the review, experiments have shown the capability of RMPs to suppress ELM, their capability to ether degrade or improve particle confinement (so-called density pump-out in the loss case), to increase the threshold to L-H transition, the increase of fluctuations and the reduction of large scale structures, etc. Concerning simulations, the impact of RMP on the plasma itself (plasma response) and ELMs has been a hot topic since the 2000s. The impact of RMPs has been studied through MHD and 3D fluid transport codes mainly [8, 9]. The self-consistent 3D modelling of their effects on turbulence has been studied at early stage by [10]. This work hopes to give some complements on the work of[10] and reflections on the turbulence developing for different amplitudes of magnetic perturbations (MP) and its consequence on the SOL density decay length λ_N. We begin by a description of the implementation of MP in a 3D electrostatic fluid code, then present the impact of single mode MP first on equilibrium then on turbulence properties. The paper ends, before the usual conclusion, with a discussion of the scope of our results.

2 Implementation of MP in the TOKAM3X code

In this presentation, we use the 3D fluid turbulence edge plasma code TOKAM3X to investigate the response of an electrostatic plasma to simple 3D RMP-like perturbations. Although TOKAM3X has the capability to solve full fluid-drift equations in complex geometries [11, 12] and non-isothermal model [13], we restrict ourselves to an isothermal model in an idealized circular limited geometry. An infinitely thin limiter is set at the High Field Side (HFS) midplane. The response of the magnetic equilibrium to the perturbation is neglected assuming the common vacuum approximation. This assumption has been the extended work of several authors[8, 14, 15] highlighting the importance of the screening of the plasma against external MP. The implementation of a plasma response is out of the scope of this paper as we consider this method to be a first step into the study of turbulence response to an idealize MP.

The magnetic field B_0 in TOKAM3X is defined in a general way as:

$$\begin{aligned}\vec{B}_0 &= \vec{\nabla} \times \left(\Psi_{\rm pol}(\psi) \vec{\nabla}\varphi + \Psi_{\rm tor}(\psi,\theta) \vec{\nabla}\theta \right) \\ &= F \vec{\nabla}\varphi + \vec{\nabla}\Psi_{\rm pol} \times \vec{\nabla}\varphi \\ &= B_0^\theta \vec{e}_\theta + B_0^\varphi \vec{e}_\varphi \end{aligned} \quad (1)$$

where the curvilinear coordinate system (ψ, θ, φ) is used. φ is the toroidal angle, θ is a curvilinear abscissa along magnetic flux surfaces in the $(R - Z)$ plan and ψ labels flux surfaces. Ψ is a flux function and $(\vec{e}_i)_{i=\psi,\theta,\varphi}$ defines the covariant basis associated to the (ψ, θ, φ) coordinates [16].

The magnetic field is then pertubated as follow:

$$\begin{aligned}\vec{B} &= \vec{\nabla} \times \left((1 + \epsilon_{\text{pol}})\Psi_{\text{pol}}\vec{\nabla}\varphi + \Psi_{\text{tor}}\vec{\nabla}\theta\right) \\ &= B^{\psi}\vec{e}_{\psi} + B^{\theta}\vec{e}_{\theta} + B^{\varphi}\vec{e}_{\varphi}\end{aligned} \tag{2}$$

With $\epsilon_{\text{pol}}(\psi, \theta, \varphi) = A\sin(m\theta - n\varphi)$. In the following, A, the magnitude, is of the order of 10^{-3}. For readable purpose the 10^{-3} part is omitted and we note $A = \alpha \cdot 10^{-3}$. The MP is thus noted (α, m, n), with α the normalized magnitude of the perturbation, m and n the poloidal and toroidal mode numbers. B^{ψ} is the new radial component of the magnetic field. Theory of magnetic perturbation ensures that the magnetic surfaces defined by a rational safety factor q resonate, forming magnetic islands (in the vaccum approximation framework, they are sometimes referred as Poincaré islands) for $q = m/n$ [2]. A Poincaré plot for $\alpha = 1$, $m = 6$ and $n = 2$ is shown in figure 1. One can notice also a chain of island at $m/n = 7/2$ due to the curvature of the toroidal geometry and the MP, which leads to the existence of additional modes.

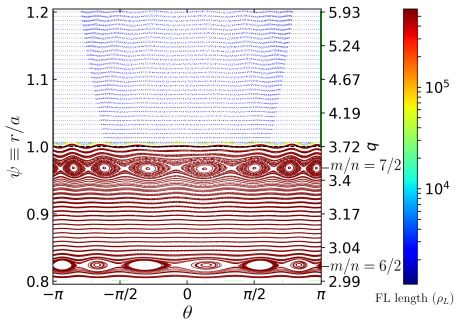

Figure 1: *Poincaré plot of the magnetic field in TOKAM3X for* $\epsilon_{pol} = 10^{-3}\sin(6\theta - 2\varphi)$

3 Impact of single mode perturbation in 3D flux driven simulations

A set of 5 simulations in limited circular geometry has been done on a $64(\psi) \times 512(\theta) \times 32(\varphi)$ meshgrid. The geometry is a half-torus with an aspect ratio $\epsilon_a = 2.45$. We set the normalized collisionality $\nu^* = \frac{\rho_L}{\tau_e c_s} = 0.01$, with ρ_L the Larmor radius, τ_e the electron collision time and c_s the thermal velocity. In the radial direction, half of the simulation box is the Scrape-off Layer (SOL) and the other half is the closed field line region (CFLR). We simulate a radial direction $r/a \equiv \psi \in [0.8; 1.2]$ with a the minor radius set at $330\rho_L$ for the simulations. The unperturbed magnetic field has a safety factor q varying from 3 in the CFLR (close to the core plasma) to 6 in the far SOL (close to the wall), following a parabolic law. The table 1 states the different MP used.

Simulation	α	m	n
Reference	0	0	0
MP	1/2	6	2
	1	6	2
	2	6	2
	3	6	2

Table 1: *Set of MP for the simulations*

3.1 Impact on equilibrium

Perturbed simulations exhibit a drop of the particle content when we plot the time evolution of particle content (figure 2), reminiscent of the density pump-out observed in experiments. The amplitude of the pump-out is of the order of 5 to 10 % and is not monotonic with the amplitude, as we observe a reverse trend for $\alpha \geq 1$.

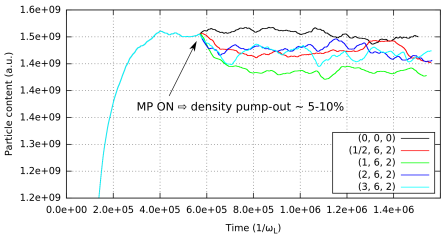

Figure 2: *Time evolution of particle content for each simulation.*

The log scale average (in (t, θ, ϕ)) density profile in the radial direction is seen on figure 3 on the left. The density gradient change seems mainly in the SOL, with non monotonic effect in view of the amplitude of the MP, but a small decrease is observed on the CFLR. As the density is largely higher in CFLR as in the SOL, the pump-out effect is mainly in the CFLR, with a loss of density in this region. We could thing that the pump-out is due to the radial component of the parallel flux whose existence is related to the new radial component of the radial magnetic field, but figure 3 on the left shows that this flux is only a neglectable part of the total radial flux ($< 1\%$ of the total radial flux).

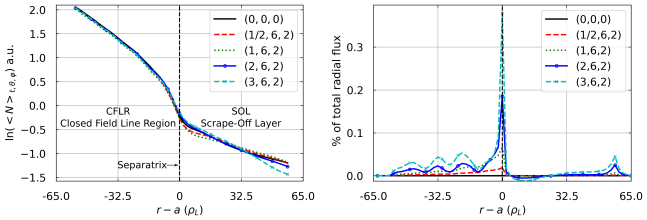

Figure 3: *Left: Radial profile of the logarithme of the density profile at LFS midplane. Right: Radial profile of the radial component of the parallel ion flux as a percentage of the total radial flux*

We continue the description of the consequences of MP with the response of the radial electric field, that is not impacted in the SOL but increases with the amplitude of the MP in the CFLR as seen in figure 4. It results in a flow reorganization as seen in the increase of the

Density decay length (in ρ_L)				
MP	$< \lambda_N >$	$\lambda_{N,\mathrm{BOT}}$	$\lambda_{N,\mathrm{LFS}}$	$\lambda_{N,\mathrm{TOP}}$
$(0,0,0)$	62	43	39	32
$(1/2,6,2)$	71 ↗	44 ∼	58 ↗	32 ∼
$(1,6,2)$	74 ↗	44 ∼	59 ↗	46 ↗
$(2,6,2)$	28 ↘	32 ↘	30 ↘	29 ∼
$(3,6,2)$	27 ↘	23 ↘	25 ↘	25 ↘

Table 2: *SOL density decay length λ_N (in Larmor radius ρ_L) averaged, at bottom, LFS midplane and top*

radial profile of the parallel Mach number $M_\parallel$ at LFS midplane on figure 4. We note a monotonic increase of $M_\parallel$ with the amplitude of the MP in the CFLR with a maximum at the separatrix. The behavior in the SOL shows a plateau for $\alpha \leq 1$ at the middle of the SOL. For $\alpha \geq 2$, $M_\parallel$ decreases linearly.

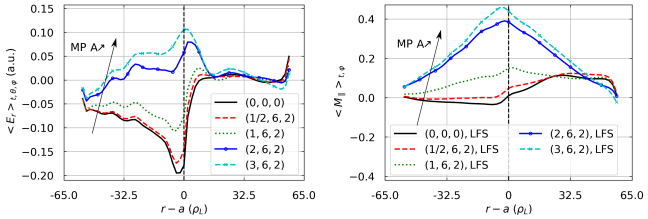

Figure 4: *Right: Mean radial electric field E^ψ averaged along (θ, φ). Left: Mean radial parallel Mach number ($M_\parallel$) at LFS midplane, averaged along (φ). $M > 0$ in ion diamagnetic direction*

Finally, the radial SOL density decay length is calculated as $\lambda_N = -N/\partial_\psi N$. The table 2 offers a quick view of λ_N at different points in the SOL for the different MP. For $\alpha \leq 1$, the radial density decay length increases a little. The trend reverses and λ_N sinks for $\alpha \geq 2$.

3.2 Impact on turbulence properties

We have seen the consequences of MP on equilibrium but the observed situation cannot be fully link between each equilibrium quantities. As for edge plasma, a large part of the physic is driven by turbulence, we study this topic in this following part.

In figure 5 a radial profile of turbulence intensity of density events σ_N/N at the LFS midplane shows an almost linear behavior at the CFLR with an increases for MP with $\alpha \geq 2$. In the SOL, the effect of MP is non monotonic. Turbulence intensity drops for $\alpha \leq 1$ and rises for ≥ 2.

Probability density functions (PDF) is used to highligh some behaviours of the density events and the structure of turbulence. For each simulation, 4 PDF along the radial direction at LFS midplane have been plotted (see figures 6). The radial positions (from left to right and top to bottom) are the middle of the CFLR ($\psi = 0.90$), just before the separatrix ($\psi = 0.98$), just after the separatrix ($\psi = 1.03$) and the middle of the SOL ($\psi = 1.1$). We notice that the shape of the PDF at $\psi = 0.90 \rightarrow 0.98$ is

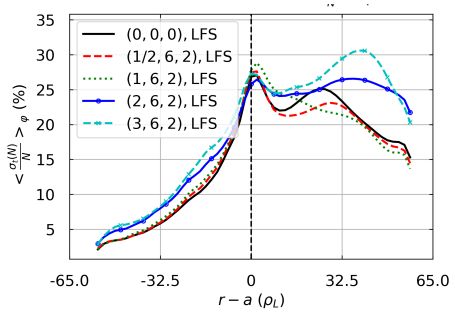

Figure 5: *Radial profile of turbulence intensity at LFS midplane as standart deviation of density normalized by density*

nearly a Gaussian for all amplitudes of MP. Just after the separatrix ($\psi = 1.03$), the shapes skew less to the right for $\alpha \leq 1$, meaning an increase of the high amplitude turbulent events. The intermittency (high amplitude events are less likely) is a caracteristic of the SOL turbulence observed experimentally [4]. This trend decreases from the case without MP until $\alpha = 1$ in the SOL with almost a bimodal distribution for this amplitude at $\psi = 1.1$ in the SOL. For $\alpha = 1$, the turbulent events seems to reach an equilibrium between low amplitude events and high amplitude events, even if the turbulence intensity shows a decreasing behavior for the same amplitude in figure5. For higher amplitudes of MP ($\alpha \geq 2$), the effect is different as a quasi Gaussian shape still appears near the separatrix. The shapes of the PDF show a higher skewness, which means the occurence of a turbulence with more intermittency (events of large amplitudes are lesser in number).

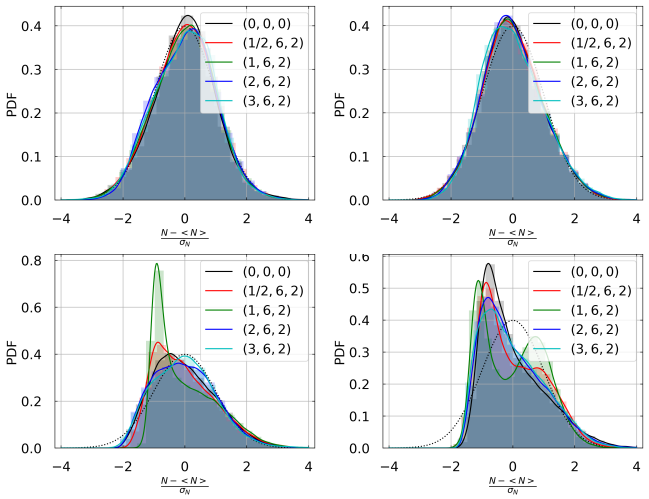

Figure 6: *Probability density functions of density fluctuation $\tilde{N}$ at (from left to right and top to bottom) $\psi = 0.90$, $\psi = 0.98$, $\psi = 1.03$, $\psi = 1.1$ at the LFS midplane. The dotted line is a standard normal distribution for help*

4 Discussion

The last section shows impact of MP on equilibrium quantities and we observe qualitatively the same trends

in experiments for some results [4, 7, 17].

The impact on turbulence is more complex. It does not scale with the amplitude of the MP as we see a reversing of the trend in the SOL for the turbulence intensity for example. For MP with $\alpha \leq 1$, the turbulence intensity decreases a little compare to the case without MP, the intermittency decreases.Turbulence intensity only increases for MP with $\alpha \geq 2$, coupling with an increase of intermittency.

For MP with $\alpha \leq 1$, the turbulence has more likely bursts of high density events (as seen in the PDF), accounting for a small increase of transport in the case $\alpha = 1$, where the pump-out is the highest of the set of simulations. It seems that a loss of intermittency with more likely high amplitude turbulent event is correlated with a increase of the pump-out amplitude, even with a loss of turbulent intensity. Maybe the high density and more likely bursts maintain a higher radial transport compare to the reference case, with more intermittency and so less likely high density bursts. The link between all these observations remain unclear.

In [18], a link is done between turbulent structures and SOL density decay length λ_N. We plot in figure 7 the time and toroidal averaged turbulence intensity of density events (left axis) and the skewness (intermittency higher for higher skewness, right axis) as a function of the SOL density decay length for each simulation at LFS midplane. It may seem, that the lower the turbulence intensity and the intermittency (with more likely high density turbulent events) are, the higher the SOL density decay length is.

In [10], MP have shown the capability to break turbulent structures. If we seem to observe a similar effect for MP $\alpha \geq 2$ (seen through the decrease of intermittency),we obtain a curious regime at amplitudes $\alpha \leq 1$, where the MP seems to couple with turbulent structures (as the λ_N increases).

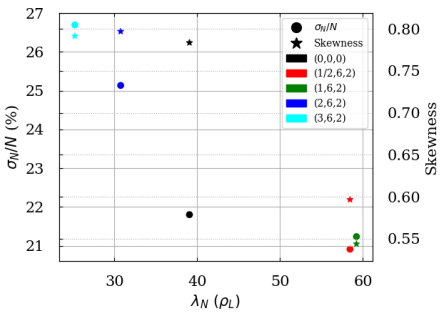

Figure 7: *Time and toroidal averaged turbulence intensity (left axis, round marker) and skewness (right axis, star marker) as a function of SOL density decay length at LFS midplane*

5 Conclusion

A 3D fluid code for edge plasma TOKAM3X has been used to study the impact of several amplitude-varying single mode MP on transport and turbulence.

Even with the simple theoritical framework chosen here (isothermal model, electrostatic, vacuum approximation, etc.), we reproduce qualitatively observations made in experiments on MAST and TEXTOR, such as the flow reequilibrium coupling with the increase of radial electric field. A moderate density pump-out with fine effects on the radial transport appears for the different studied amplitudes of perturbation. This pump-out does not seem to be correlated with the increase of the perpendicular component of the parallel transport, as this increase remains neglectable, unexpectatedly.

The turbulence intensity of density events is not monotonic with the amplitude of the perturbation and we observe a reverse effect of the density pump-out at some point. This could be correlated with the increase of intermittency as the amplitude of the perturbation grows. A correlation is seen on turbulence intensity, intermittency and the SOL density decay length. About SOL density decay length we see that MP has a trend to decrease the former, only when the amplitude of the MP is high enough to increase the turbulence intermittency, with large density events becoming less likely. This last effect remains to be analyzed carefully.

6 Aknowledgement

The author would like to thank M. Peret for helpful discussions on turbulence in egde plasma.
This work was supported by the EUROfusion - Theory and Advanced Simulation Coordination (E-TASC) and has received funding from the Euratom research and training programme 2019-2020 under grant agreement No 633053. The views and opinions expressed herein do not necessarily reflect those of the European Commission. This work has been carried out thanks to the support of the A*MIDEX project (ANR-11-IDEX-0001-02) funded by the 'Investissements d'Avenir' French Government program, managed by the French National Research Agency (ANR). This work was granted access to the HPC resources of IDRIS under the allocations A0030506912 & A0050506912 made by GENCI, of Aix-Marseille University, financed by the project Equip@Meso (ANR-10-EQPX-29-01), and of the EUROfusion High Performance Computer (Marconi-Fusion) under the project HEAT.

References

[1] Allen H Boozer. *Nucl. Fusion*, 55:025001, 2015.
[2] TE Evans. *Plasma Phys. Control. Fusion*, 57:123001, 2015.
[3] Eric Nardon et al. *Jour. Nucl. Materials*, 363:1071–1075, 2007.
[4] P Tamain et al. *Plasma Phys. Control. Fusion*, 52:075017, 2010.
[5] AJ Thornton et al. *Nucl. Fusion*, 54(6):064011, 2014.
[6] R Scannell et al. *Plasma Phys. Control. Fusion*, 57(7):075013, 2015.
[7] S Mordijck et al. *Plasma Physics and Controlled Fusion*, 58(1):014003, 2015.
[8] M Becoulet et al. *Nucl. Fusion*, 52:054003, 2012.
[9] H Frerichs et al. *Phys. Plasmas*, 23(6):062517, 2016.
[10] D Reiser. *Phys. Plasmas*, 14:082314, 2007.
[11] Patrick Tamain et al. *Jour. Comp. Phys.*, 321:606–623, 2016.
[12] Davide Galassi et al. *Fluids*, 4(1):50, 2019.
[13] Camille Baudoin et al. *Cont. Plasma Phys.*, 58(6-8):484–489, 2018.
[14] Richard Fitzpatrick. *Phys. Plasmas*, 5:3325–3341, 1998.
[15] Eric Nardon et al. *Phys. Plasmas*, 14:092501, 2007.
[16] WD D'haeseleer, WNG Hitchon, JD Callen, and JL Shohet. *Flux Coordinates and Magnetic Field Structure*. Springer, 1991.
[17] JW Coenen et al. *Nucl. fusion*, 51:063030, 2011.
[18] Nicolas Fedorczak et al. *Nucl. Materials and Energy*, 12:838–843, 2017.